Regularized Blind Deconvolution using Recursive Inverse Filtering

Michael K. Ng[1]*, Robert J. Plemmons[2]**, and Sanzheng Qiao[3]***

[1] ACSys, Computer Sciences Laboratory, Research School of Information Sciences and Engineering, The Australian National University, Canberra, ACT 0200, Australia. E-mail: mng@cslab.anu.edu.au

[2] Department of Mathematics and Computer Science, Wake Forest University, Winston-Salem, NC 27109. E-mail: plemmons@wfu.edu

[3] Department of Computer Science and Systems, McMaster University, Hamilton, Ontario L8S 4K1, Canada. E-mail: qiao@maccs.dcss.mcmaster.ca

Abstract. Image restoration involves the removal or minimization of degradation (blur, clutter, noise, etc.) in an image using a priori knowledge about the degradation phenomena. Blind restoration is the process of estimating both the true image and the blur from the degraded image characteristics, using only partial information about degradation sources and the imaging system. Our main interest concerns optical image enhancement, where the degradation involves a convolution process. When an otherwise collimated, coherent beam of light encounters a turbulent flow field that includes density fluctuations, its optical wavefront becomes aberrated causing the beam to be degraded. Only partial a priori knowledge about the degradation phenomena in aero-optics is generally known, so here the use of blind deconvolution methods is essential. In this paper we provide a method to incorporate truncated eigenvalue and total variation regularization into a nonlinear recursive inverse filter blind deconvolution scheme first proposed by Kundur and Hatzinakos. We call our approach the nonnegativity and support regularized recursive inverse filter (NSR-RIF) algorithm. Simulation tests are reported on optical imaging problems.

1 Introduction

A fundamental issue in image restoration is blur removal in the presence of observation noise. Noise (sometimes more appropriately called "clutter" in images) may come, for example, as the result of thermal effects, measurement errors, digitation, or may be introduced by a recording or transmission medium. In the important case where the blurring operation is spatially invariant, i.e., it operates uniformly across the object domain, then the basic restoration computation

* Research supported by the Cooperative Research Centre for Advanced Computational Systems (ACSys).

** Research sponsored by the Air Force Office of Scientific Research and by the National Science Foundation.

*** Research supported by the Natural Sciences and Engineering Council of Canada.

involved is simply a deconvolution process that faces the usual difficulties associated with ill-conditioning in the presence of noise [4, 20]. Such a situation often occurs, for example, in imaging through atmospheric turbulence. In particular, the problem of imaging through a medium is encountered in many important situations, from astronomy to medicine.

The image observed from a shift invariant linear blurring process, such as an optical system, is described by how the system blurs a point source of light into a larger image. The image of a point source is called the *point spread function* PSF, which we denote by h. The observed image g is then the result of convolving the PSF h with the "true" image, say f. This blurring process is represented by the convolution equation

$$g = h \star f. \tag{1}$$

The standard deconvolution problem is to recover the image f from (1), given the observed image g and the blurring operator h. This basic problem appears in many forms in signal and image processing. There is much interest in removing blur and noise degradations from 1-D chemical spectra, as well as 2-D images from microscopes, telescopes, photographs, CT or MRI scanners, satellite sensors, and scintigrams (nuclear medicine images) [4, 20].

The PSF of an imaging system can sometimes be described by a mathematical formula, e.g., in the case of an out-of-focus lens system. More often, the PSF must be estimated empirically. Empirical estimates of the PSF can sometimes be obtained by imaging a relatively bright, isolated point source. In astro-imaging the point source might be a natural guide star or a guide star artificially generated using range-gated laser backscatter, e.g, [2, 6, 12, 16, 23]. Notice here that the PSF as well as the image may be degraded by noise.

In many applications data corresponding to h is not completely known. *Blind deconvolution* is the process of estimating both the true image f and the blur h from the degraded image g. The purpose of this paper is to incorporate regularization into and refine a nonlinear recursive inverse filter blind deconvolution method first proposed by Kundur and Hatzinakos [17, 18, 19]. They call their scheme the *nonnegativity and support constrained, recursive inverse filtering method*, or NAS-RIF, for short.

Applications of blind image deconvolution in optics abound in science and engineering [4, 6, 8, 16, 20]. Our work to enhance the quality of optical images has applications in defense, and to civilian technology, including astronomical imaging, e.g., [6, 16, 22, 24].

An algorithm for one dimensional regularized iterative blind deconvolution using truncated eigenvalue and total variation regularization in conjunction with recursive inverse filtering is developed in §2. We apply regularization to the inverse filter by using an inexpensive *eigenvalue truncation* scheme, and allow the user the option of applying *total variation regularization* to the estimated image. The method is extended to two dimensional imaging problems in §3. We call our approach the *nonnegativity and support regularized recursive inverse filter* (NSR-RIF) algorithm. Preliminary numerical tests are reported in §4 on some simulated optical imaging problems, and a comparison is made with the

NAS-RIF algorithm.

2 One Dimensional Deconvolution

We begin with the one dimensional signal restoration problem, which we term as image restoration in order to be consistent with terminology used later in this paper. Consider an image vector

$$f = (f_1, ..., f_n)^T, \qquad f_i \geq 0, \quad \text{for} \quad 1 \leq i \leq n,$$

and a blurring operator, or point spread function, represented by a $(2m+1)$-by-1 vector

$$h = (h_{-m}, ..., h_0, ..., h_m)^T.$$

Assuming $2m < n$, we can write the observed image g as the convolution of h and f, as given in (1). The standard deconvolution problem is to recover the image f from (1), given the observed image g and the blurring operator h. Blind deconvolution is the process of estimating both the true image f and the blur h from the degraded image g.

Writing (1) in discrete, i.e., matrix form, we have

$$g = Hf \tag{2}$$

where the convolution matrix

$$H = \begin{pmatrix} h_{-m} & & & & 0 \\ \vdots & \ddots & & & \\ h_m & \ddots & h_{-m} & & \\ & \ddots & \ddots & \ddots & \\ & & h_m & \ddots & h_{-m} \\ & & & \ddots & \vdots \\ 0 & & & & h_m \end{pmatrix} \tag{3}$$

is $(n+2m)$-by-n and column circulant. Note that H is rectangular. So, we embed H in a square circulant matrix

$$C = (H_1 \ H \ H_2) \tag{4}$$

where both

$$H_1 = \begin{pmatrix} h_0 & \cdots & h_{-m+1} \\ h_1 & \cdots & h_{-m+2} \\ \vdots & \ddots & \vdots \\ h_m & \ddots & h_1 \\ 0 & \ddots & \vdots \\ \vdots & \ddots & h_m \\ 0 & \ddots & 0 \\ h_{-m} & \ddots & \vdots \\ \vdots & \ddots & 0 \\ h_{-1} & \cdots & h_{-m} \end{pmatrix} \quad \text{and} \quad H_2 = \begin{pmatrix} h_m & \cdots & h_1 \\ 0 & \ddots & \vdots \\ \vdots & \ddots & h_m \\ 0 & \ddots & 0 \\ h_{-m} & \ddots & \vdots \\ \vdots & \ddots & 0 \\ h_{-1} & \ddots & h_{-m} \\ \vdots & \ddots & \vdots \\ h_{m-2} & \cdots & h_{-1} \\ h_{m-1} & \cdots & h_0 \end{pmatrix}$$

are $(n+2m)$-by-m and column circulant. Thus

$$H = C \begin{pmatrix} 0 \\ I_n \\ 0 \end{pmatrix}.$$

Correspondingly, we can embed f in an $(n+2m)$-by-1 vector

$$\tilde{f} = \begin{pmatrix} \tilde{f}_a \\ \tilde{f}_b \\ \tilde{f}_c \end{pmatrix} = \begin{pmatrix} 0 \\ f \\ 0 \end{pmatrix}$$

where 0 in the last vector represents an m-by-1 null vector. Then (2) is equivalent to

$$g = C\tilde{f}. \tag{5}$$

Equation (5) is called the extended sequence convolution form of (2) and leads to the *extended sequence deconvolution method* [15]. Here, (5) is often preferable to (2), because its coefficient matrix C is a square circulant matrix, which has many desirable properties. For example, if H in (3) has full column rank, then C is invertible and its inverse is also circulant and C^{-1} can be efficiently computed using the fast Fourier transform (FFT), yielding the extended sequence deconvolution method for computing f.

In blind deconvolution, we are given the observed image g. To estimate f and H using (2), we need to estimate the length (extent, or support) n of the true image f. The bandwidth $2m+1$ of H can then be found using n and the length of g. Similarly, if we use (5) to estimate $\tilde{f}$ and C, we also need to know the size n of the nonzero vector f in $\tilde{f}$. The structure of C can then be determined by n and the length of g. Thus, the size of the true image, called the support constraint, is crucial information in blind deconvolution using either (2) or (5). In addition to the support constraint on f, nonnegativity of the pixel values, represented by the f_i, is an important requirement. This is called the *nonnegativity constraint*, and can be incorporated into deconvolution computations [4, 20]. Assuming that C is invertible, we can formulate the blind deconvolution problem as:

Find C (or the first column of C) such that $\tilde{f} = C^{-1}g$ with $\tilde{f}_a = \tilde{f}_c = 0$ and $\tilde{f}_b \geq 0$.

2.1 Iterative Blind Deconvolution

Some iterative blind deconvolution methods begin with a knowledge-based (non-negativity, finite support) estimate for f, "deconvolve" $g = h \star f$ to estimate h, and then iterate in an alternating fashion to improve the estimates for both f and h [5, 8, 29]. These methods involve variations of direct, rather than inverse, filtering. Kundur and Hatzinakos [17, 18, 19], however, have recently presented a novel blind deconvolution method using recursive *inverse filtering.* Inverse filters are easier to implement and avoid certain inversion procedures, thus reducing the computational complexity.

The method by Kundur and Hatzinakos uses a variable finite impulse response (FIR) filter of length $2p+1$, where p is an estimate for m in H in (3), characterized by its parameter vector:

$$u = (u_{-p}, ..., u_0, ..., u_p)^T, \tag{6}$$

and the process iterates with respect to u. The observed image g is the input to the filter. The output is the convolution of u and g: $y = u \star g$, which is then constrained and used to approximate the true image f. Assuming the length of g is k, we can write the convolution in matrix form:

$$y = Ug,$$

where the convolution matrix

$$U = \begin{pmatrix} u_{-p} & & & & 0 \\ \vdots & \ddots & & & \\ u_p & \ddots & u_{-p} & & \\ & \ddots & \ddots & \ddots & \\ & & u_p & \ddots & u_{-p} \\ & & & \ddots & \vdots \\ 0 & & & & u_p \end{pmatrix} \tag{7}$$

is a $(k+2p)$-by-k banded Toeplitz matrix of bandwidth $2p+1$. The output y is then passed through a nonlinear filter which maps y to $\tilde{y}$ such that $\tilde{y}$ has a finite support, say n, and is nonnegative. Specifically, assuming that we choose p so that $r = (k+2p-n)/2$ is an integer and denoting $P_n = \mathrm{diag}(p_i)$ where

$$p_i = \begin{cases} 1, & \text{if } y_{r+i} > 0; \\ 0, & \text{otherwise;} \end{cases} \qquad \text{for} \quad 1 \leq i \leq n,$$

we get, in matrix form,

$$\tilde{y} = \begin{pmatrix} 0 & 0 & 0 \\ 0 & P_n & 0 \\ 0 & 0 & 0 \end{pmatrix} y.$$

In other words, the nonlinear filter sets any component which is either outside the finite support or is negative, to zero. The resulting vector $\tilde{y}$ is an estimate for the true nonnegative image with support n. That is

$$\tilde{y} \approx \tilde{f}.$$

The error vector is given by

$$z = y - \tilde{y} = \begin{pmatrix} I_r & 0 & 0 \\ 0 & I_n - P_n & 0 \\ 0 & 0 & I_r \end{pmatrix} y \equiv Dy. \tag{8}$$

The parameter vector u in (6) for our FIR filter is determined by minimizing the error $\|z\|_2^2$. In order to avoid a trivial null vector u, an additional term

$$\gamma(\sum_{i=-p}^{p} u_i - 1)^2 = \gamma(e^T u - 1)^2$$

is incorporated into the objective function, where $\gamma \geq 0$ and $e = (1, ..., 1)^T$. Specifically, the objective function is

$$J(u) = \|z\|_2^2 + \gamma(e^T u - 1)^2. \tag{9}$$

An optimal FIR filter is found by minimizing the above objective function $J(u)$. It is proved in [19] that $J(u)$ is convex. Thus the global minimum exists and a variety of numerical optimization algorithms can be used to compute u minimizing $J(u)$. Kundur and Hatzinakos [17, 18, 19] use a nonlinear conjugate gradient method to search for the minimum. Thus they call their algorithm the *nonnegativity and support constraints recursive inverse filter* (NAS-RIF).

As described above, in matrix terminology, Kundur and Hatzinakos use a banded Toeplitz matrix U of the form (7) to approximate the deconvolution matrix. Recalling that k is the length of the input image vector g and $2p + 1$ is the filter length, their deconvolution matrix is a $(k + 2p)$-by-k banded Toeplitz matrix of lower bandwidth $2p + 1$.

Using the circulant matrix C representation, we propose to use a k-by-k circulant matrix, which we call S, to approximate the inverse of C. Of course the inverse of a circulant matrix is circulant. Specifically, we let S be the k-by-k circulant matrix with first column

$$(s_0, ..., s_p, 0, ..., 0, s_{-p}, ..., s_{-1})^T, \quad 1 \leq p < \frac{k}{2} \tag{10}$$

where p is an estimate for m in H in (3), and denote

$$S = Circ[(s_0, ..., s_p, 0, ..., 0, s_{-p}, ..., s_{-1})^T].$$

Thus, the FIR filter performs a multiplication of the circulant matrix S and the observed image g. This multiplication can be implemented efficiently using the FFT. Note that the output of the filter is a k-by-1 vector, whereas in NAS-RIF the output is $(k+2p)$-by-1. The output $y = Sg$ is sent to the nonlinear filter and mapped to $\tilde{y}$ satisfying the nonnegativity and support constraints. Then the error $z = y - \tilde{y}$ is measured and fed back to compute an adjustment to the FIR parameter vector u to reduce the value of the objective function $J(u)$. This procedure is iterated until the objective function reaches the global minimum, or some early stopping criteria applies.

2.2 Regularizing Iterative Blind Deconvolution

Continuous deconvolution can be modeled as an integral equation of the first kind (an ill-posed inverse problem [7, 9]). It is well-known that deconvolution algorithms can be extremely sensitive to noise [4, 15]. For example, if the noise is additive, then the blurring process can be represented by a convolution equation of the form

$$g = h \star f + \eta,$$

which, by (5), is equivalent to

$$g = C\tilde{f} + \eta. \tag{11}$$

Assuming that C is invertible, from (11) we have

$$C^{-1}g = \tilde{f} + C^{-1}\eta.$$

In applications arising from integral equations of the first kind, the ill-conditioning of C stems from the wide range of the magnitudes of its eigenvalues [7, 9]. Therefore, excess amplification of the noise at small eigenvalues can occur. Figure 1 shows a practical example of a 2-dimensional discrete point spread function from [22] in atmospheric imaging, with a general Gaussian form [15]. Figure 2 depicts the distribution of the magnitudes $|\lambda_i|$ of the eigenvalues of the convolution matrix C corresponding to the point spread function in Figure 1. We see that many of the $|\lambda_i|$ are relatively small.

Since any realistic signal processing problem involves noise, it is necessary to incorporate regularization into deconvolution to stablize the computation [7, 9, 13, 14]. Regularization methods attempt to alleviate sensitivity to the noise by "filtering" out eigen-components of the solution belonging to the noise subspace. For some iterative methods, it has been established that early termination of the iterations accomplishes this regularization effect. That is, the eigen-components of the signal subspace are reconstructed in the first (possibly many) iterations and, after reaching a certain approximate restoration, the components in the noise subspace begin to be reconstructed. It is at this point, where the noise begins to contaminate the reconstruction, that the iterations are halted, see, e.g., Hanke and Hansen [10].

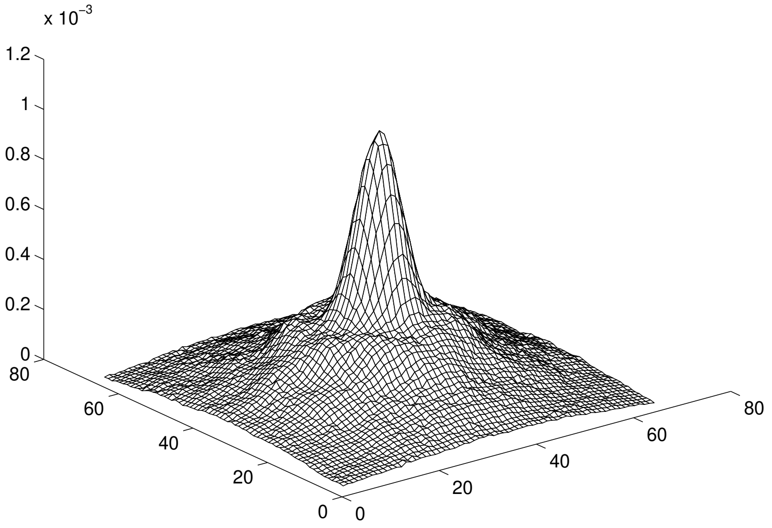

Fig. 1. Example of a discrete 2-D Gaussian blur point spread function (64×64)

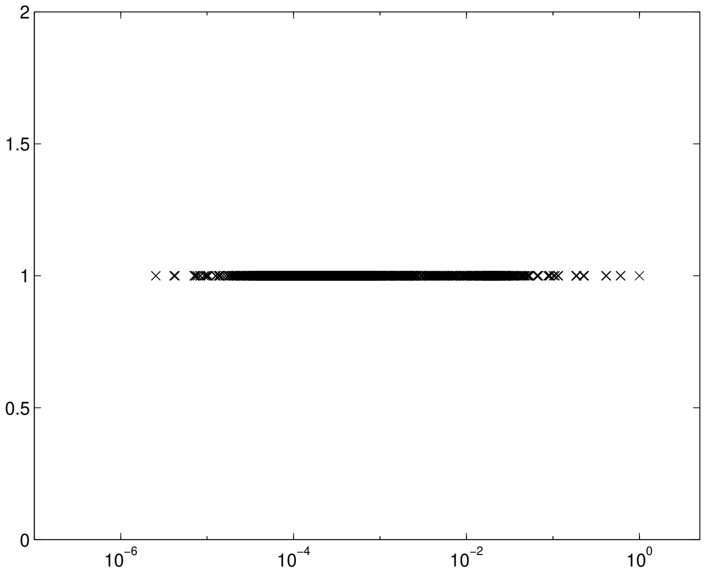

Fig. 2. Distribution of the $|\lambda_i|$ for the 129×129 convolution matrix C with the PSF given in Figure 1

The simulations by Kundur and Hatzinakos [18] show that their NAS-RIF algorithm is sensitive to noise and, in fact, amplifies noise. The regularization method they employ is that of truncated iterations.

Now, we describe an alternative regularization procedure for the NAS-RIF algorithm. Our proposed method is referred to as the *nonnegativity and support constraints regularized recursive inverse filter* (NSR-RIF). The idea is to apply regularization to the inverse filter by using an inexpensive *eigenvalue truncation* scheme.

Recall that the vector

$$(s_0, ..., s_p, 0, ..., 0, s_{-p}, ..., s_{-1})^T$$

is the first column of the circulant matrix S which is an estimate for C^{-1}. Since S is circulant, its eigenvalues can be efficiently computed using the DFT. Specifically, if F is the k-by-k Fourier matrix, i.e., its entries are given by

$$[F]_{j,\ell} = \frac{1}{\sqrt{k}} e^{-2\pi i j \ell / k}, \quad 0 \leq j, \ell \leq k-1,$$

where $i = \sqrt{-1}$. Then the vector

$$\hat{s} = F(s_0, ..., s_p, 0, ..., 0, s_{-p}, ..., s_{-1})^T$$

contains the eigenvalues of S. Using the FFT, we can obtain the eigenvalues in $O(k \log k)$ operations. To incorporate regularization into deconvolution to stablize the computation, we need to penalize the small, in magnitude, eigenvalues of the convolution matrix C. Equivalently, in our inverse filter, we suppress the large, in magnitude, eigenvalues of the deconvolution matrix S as follows. We first apply a nonlinear filter represented by a k-by-k matrix Q:

$$\tilde{s} = Q\hat{s}$$

where $Q = \mathrm{diag}(q_i)$ and

$$q_i = \begin{cases} 1, & \text{if } |\hat{s}_i| \leq \tau; \\ 0, & \text{otherwise}; \end{cases} \qquad \text{for} \quad 1 \leq i \leq k,$$

where τ is a predetermined tolerance. In other words, the nonlinear filter characterized by Q sets all the eigenvalues whose absolute values are greater than τ to zero. Effectively, the regularization is achieved by truncating the small eigenvalues of S^{-1}, which is an estimate for the convolution matrix C. Then we measure the error

$$v = \hat{s} - \tilde{s} = (I - Q)\hat{s} \equiv B\hat{s}$$

and incorporate this error into the objective function $J(u)$ given by (9). Specifically, let

$$s = (s_{-p}, ..., s_{-1}, s_0, ..., s_p)^T$$

be the filter parameter vector, then our regularized objective function is reformulated now in terms of s as

$$J_{reg}(s) \equiv \|z\|_2^2 + \mu\|v\|_2^2 + \gamma(e^T s - 1)^2, \tag{12}$$

recalling that z is the error vector $y - \tilde{y}$. The parameter μ in (12) controls the degree of regularization. The filter parameter vector s is determined by minimizing our new objective function (12). Figure 3, which also involves regularization of the image calculation as described in Section 2.3, gives an overview of our overall scheme.

Now we consider the gradient of J_{reg}. Using the following equations

$$\begin{pmatrix} s_0 \\ \vdots \\ s_p \\ 0 \\ \vdots \\ 0 \\ s_{-p} \\ \vdots \\ s_{-1} \end{pmatrix} = \begin{pmatrix} 0 & I_{p+1} \\ 0 & 0 \\ I_p & 0 \end{pmatrix} \begin{pmatrix} s_{-p} \\ \vdots \\ s_{-1} \\ s_0 \\ \vdots \\ s_p \end{pmatrix}, \qquad D^T D = D, \qquad B^T B = B,$$

we can show that the gradient of $J_{reg}(s)$ is

$$\nabla J_{reg}(s) = 2Gz + 2\mu \mathrm{Re}(E^H v) + 2\gamma(e^T s - 1)e \tag{13}$$

where G is a $(2p+1)$-by-k row-circulant matrix with its first row:

$$(g_{p+1}, g_{p+2}, \ldots, g_k, g_1, \ldots, g_p),$$

and

$$E = F \begin{pmatrix} 0 & I_{p+1} \\ 0 & 0 \\ I_p & 0 \end{pmatrix}.$$

Since G is row-circulant and F is the k-by-k Fourier matrix, the gradient can be computed efficiently. Furthermore, we can show that $J_{reg}(s)$ is convex.

Theorem 1. *Let $J_{reg}(s)$ be twice differentiable in $R^{(2p+1)}$. Then J_{reg} is convex for all s in $R^{(2p+1)}$ if the Hessian $\nabla^2 J_{reg}(s)$ is positive semi-definite, and is strictly convex if the Hessian is positive definite.*

From (13), it can be shown that the Hessian of the objective function is given by

$$\nabla^2 J_{reg}(s) = 2GDG^T + 2\mu \mathrm{Re}(E^H BE) + 2\gamma ee^T, \tag{14}$$

leading to the convexity result for $J_{reg}(s)$, by Theorem 1. Thus the global minimum exists and a variety of numerical optimization algorithms can be used to compute s minimizing $J_{reg}(s)$. In our numerical examples, a nonlinear conjugate gradient method is used to search for the global minimum.

Our basic regularized iterative blind deconvolution algorithm is listed in Table 1. Figure 3 summarizes the method and also shows how additional regularization of the estimated image can be incorporated into the scheme, according to the method proposed in §2.3.

2.3 Regularizing the Estimated Image

In this section, we propose a regularization method for the image estimated by our NSR-RIF algorithm given in Table 1. This image regularization method can also be incorporated into the NAS-RIF by Kundur and Hatzinakos [17, 18, 19] to improve their restored image.

The image $\tilde{y}$ estimated by the NSR-RIF satisfies the nonnegativity and support constraints. Let $\tilde{a}$ be the nonnegative segment of size n at the center of $\tilde{y}$, i.e.,

$$\tilde{a} = (0 \quad I_n \quad 0)\tilde{y}.$$

In the one-dimensional case, we perform the regularization by solving for

$$a = (a_1, ..., a_n)^T$$

in the following penalized least squares minimization problem:

$$\min_a \left\{ \frac{1}{2}\|\tilde{a} - a\|_2^2 + \alpha \sum_{k=1}^{n-1} \sqrt{|a_{i+1} - a_i|^2 + \beta} \right\}$$

where $\alpha > 0$ controls the degree and $\beta(\geq 0)$ controls the variability of the penalty term. When $\beta = 0$ we have the usual *total variation minimization*, which has been studied extensively in recent years, e.g., [1, 5, 25, 26, 27, 28]. It is known that this approach is especially effective in preserving *sharp* edges. Similarly, total variation has the advantage that it does not penalize *smooth* images. On the other hand, disadvantages include the complexity level in solving total variation minimization problems, and the fact that minimizing the variation of the pixel values a_i can sometimes cause a loss of fine detail in the image [7]. For these reasons we leave the incorporation of total variation regularization of the estimated image as a user option in our NSR-RIF scheme (see Figure 3).

Suppose that a is the solution of above minimization problem. The gradient of the associated objective function at a is

$$a + \alpha A_\beta(a)a - \tilde{a},$$

where $A_\beta(a)$ is a symmetric and tridiagonal matrix with its subdiagonal

$$\begin{pmatrix} -\frac{1}{\sqrt{|a_2-a_1|^2+\beta}} \\ \vdots \\ -\frac{1}{\sqrt{|a_n-a_{n-1}|^2+\beta}} \end{pmatrix},$$

and its diagonal

$$\begin{pmatrix} \frac{1}{\sqrt{|a_2-a_1|^2+\beta}} \\ \frac{1}{\sqrt{|a_2-a_1|^2+\beta}} + \frac{1}{\sqrt{|a_3-a_2|^2+\beta}} \\ \vdots \\ \frac{1}{\sqrt{|a_{n-1}-a_{n-2}|^2+\beta}} + \frac{1}{\sqrt{|a_n-a_{n-1}|^2+\beta}} \\ \frac{1}{\sqrt{|a_n-a_{n-1}|^2+\beta}} \end{pmatrix}.$$

Thus the minimizer a is the solution of the following equation

$$(I_n + \alpha A_\beta(a))a = \tilde{a}.$$

We make two observations: first, $I_n + \alpha A_\beta(a)$ is an M-matrix (see e.g., Berman and Plemmons [3]). Thus the entries of the inverse of $(I_n + \alpha A_\beta(a))$ are nonnegative. Second, a is the result of two consecutive mappings on the filter output y, first nonnegativity and support and then total variation regularization. These two observations ensure the nonnegativity of a.

We remark that the regularized image estimate a can replace $\tilde{y}$ as an input to compute the error vector z in the recursive inverse filter algorithm. The switch in Figure 3 indicates this option.

3 2-D Problems: Atmospheric Blurring

The results of §2 extend in a natural way to 2-D image blind deconvolution. Our main interest concerns optical image enhancement. Applications of blind image deconvolution in optics can be found in many areas of science and engineering, e.g, see the recent book by Roggemann and Welsh [24]. This work to enhance the quality of optical images has applications in defense, and to civilian technology, including astronomical and medical imaging. Only partial a priori knowledge about the degradation phenomena or PSF in aero-optics is generally known, so here the use of blind deconvolution methods is essential. In addition, the estimated PSF is generally degraded in a manner similar to that of the observed image.

If we let $\mathcal{H}$ denote the blurring operator and η the noise process, then the image restoration problem, for example with additive noise, can be expressed as a linear operator equation

$$g = \mathcal{H}f + \eta, \tag{15}$$

where g and f denote functions containing the information of the recorded and original images, respectively. Let v and w denote two-dimensional variables. If $\mathcal{H}$ is a convolution operator, as is often the case in optical imaging, then the operator acts uniformly (i.e., in a spatially invariant manner) on f. Here, (15) can be written as

$$(\mathcal{H}f)(x) = \int h(x-y)f(y)dy. \tag{16}$$

After discretization of (15), the spatial operator $\mathcal{H}$ defined by h in (16) is a matrix that we denote by H. In this section we consider numerical methods for approximating the solution to the linear restoration problem in discretized (matrix) form obtained from the operator equation given in (15), namely:

$$g = Hf + \eta. \tag{17}$$

For notation purposes we assume that the image is n-by-n, and thus contains n^2 pixels. Typically, n is chosen to be a power of 2, such as 256 or larger. Then

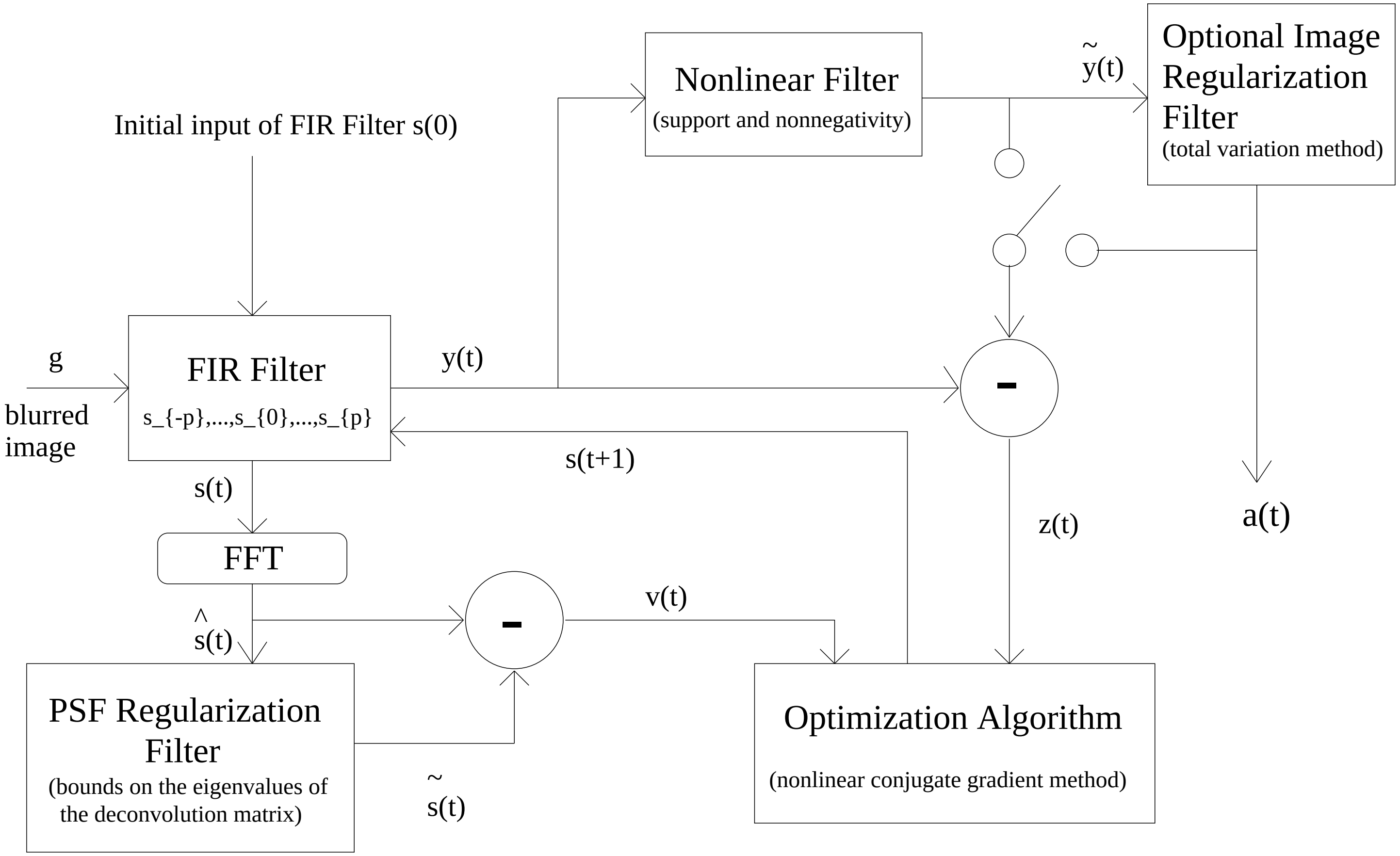

Fig. 3. NSR-RIF Algorithm

the number of unknowns grows to at least 65,536. The vectors f, g represent the observed and true image pixel values, respectively, unstacked by rows.

In the spatially invariant case generally assumed for atmospherically blurred images (as well as other applications [4, 15, 20, 24]), the blurring operates uniformly across the two dimensional image of the object in question, i.e.,

$$h(i, j; k, \ell) = h(i - k, j - \ell).$$

Here the convolution matrix H is a block column-circulant matrix with column-circulant blocks. More precisely,

$$H = \begin{pmatrix} H^{(-m_y)} & & & 0 \\ H^{(-m_y+1)} & H^{(-m_y)} & & \\ \vdots & \ddots & \ddots & \\ H^{(0)} & \ddots & \ddots & H^{(-m_y)} \\ \vdots & \ddots & \ddots & H^{(-m_y+1)} \\ H^{(m_y-1)} & \ddots & \ddots & \vdots \\ H^{(m_y)} & \ddots & \ddots & H^{(0)} \\ & H^{(m_y)} & \ddots & \vdots \\ & & \ddots & H^{(m_y-1)} \\ 0 & & & H^{(m_y)} \end{pmatrix} \tag{18}$$

with each subblock $H^{(j)}$ being a $(n + 2m_x)$-by-n matrix of the form given by (3). The dimensions of the discrete point spread function h are m_x and m_y in the x-direction and y-direction, respectively.

We can embed H in a square *block-circulant-circulant-block* (BCCB) matrix

$$C = (C_1 \ C_2 \ C_3)$$

where

$$C_2 = \begin{pmatrix} C^{(-m_y)} & & & 0 \\ C^{(-m_y+1)} & C^{(-m_y)} & & \\ \vdots & \ddots & \ddots & \\ C^{(0)} & \ddots & \ddots & C^{(-m_y)} \\ \vdots & \ddots & \ddots & C^{(-m_y+1)} \\ C^{(m_y-1)} & \ddots & \ddots & \vdots \\ C^{(m_y)} & \ddots & \ddots & C^{(0)} \\ & C^{(m_y)} & \ddots & \vdots \\ & & \ddots & C^{(m_y-1)} \\ 0 & & & C^{(m_y)} \end{pmatrix},$$

$$C_1 = \begin{pmatrix} C^{(0)} & \cdots & C^{(-m_y+1)} \\ C^{(1)} & \cdots & C^{(-m_y+2)} \\ \vdots & \ddots & \vdots \\ C^{(m_y)} & \ddots & C^{(1)} \\ 0 & \ddots & \vdots \\ \vdots & \ddots & C^{(m_y)} \\ 0 & \ddots & 0 \\ C^{(-m_y)} & \ddots & \vdots \\ \vdots & \ddots & 0 \\ C^{(-1)} & \cdots & C^{(-m_y)} \end{pmatrix} \quad \text{and} \quad C_3 = \begin{pmatrix} C^{(m_y)} & \cdots & C^{(1)} \\ 0 & \ddots & \vdots \\ \vdots & \ddots & C^{(m_y)} \\ 0 & \ddots & 0 \\ C^{(-m_y)} & \ddots & \vdots \\ \vdots & \ddots & 0 \\ C^{(-1)} & \ddots & C^{(-m_y)} \\ \vdots & \ddots & \vdots \\ C^{(m_y-2)} & \cdots & C^{(-1)} \\ C^{(m_y-1)} & \cdots & C^{(0)} \end{pmatrix}.$$

Here each subblock $C^{(j)}$ is a $(n+2m_x)$-by-$(n+2m_x)$ matrix of the form given by (4).

Following the BCCB matrix C representation, we use a $(n+2m_y)(n+2m_x)$-by-$(n+2m_y)(n+2m_x)$ BCCB matrix deconvolution matrix S to approximate the inverse of C. Note that the inverse of a BCCB matrix is also BCCB and is thus completely specified by its first column. Hence the inverse FIR filter vector is completely determined by the first column of the deconvolution matrix S.

In the extension of our NSR-RIF algorithm, we perform a multiplication of the circulant matrix S and the stacked, observed image g using the two dimensional fast Fourier transform (2-D FFT). The output y is sent to the nonlinear filter and mapped to $\tilde{y}$ to satisfy the nonnegativity and support constraints. The output, $\hat{s}$, of the 2-D FFT of the first column of S is sent to the nonlinear filter and mapped to $\tilde{s}$ for regularization. The errors $z = y - \tilde{y}$ and $v = \hat{s} - \tilde{s}$ are measured and fed back to compute an adjustment to the FIR parameter vector to reduce the value of the objective function. This procedure is iterated until the objective function reaches the global minimum, or some early stopping criteria applies. The regularization scheme for the estimated image described in §2.3 also extends to 2-D case in a natural way.

3.1 Guide Star Image

In two dimensional deconvolution problems arising in ground-based atmospheric imaging, a primary objective is to remove the blurring in an image resulting from the effects of atmospheric turbulence. The problem consists of an n-by-n image, received by a ground-based imaging system together with an n-by-n image of a guide star PSF, observed under similar circumstances. Empirical estimates of the PSF can sometimes be obtained by imaging a relatively bright, isolated point source. In astro-imaging the point source might be a natural guide star or a guide star artificially generated using range-gated laser backscatter, e.g, [2, 12, 23]. Notice here that the PSF as well as the image may be degraded by noise.

The imaging system detects the atmospheric distortions, represented by the PSF, using the guide star image. A wavefront sensor measures the optical distortions which can then be digitized into a blurred image of the guide star pixels. To form an initial estimate of the PSF, the rows of the blurred pixel guide star image are stacked into a column vector. The 2-D FFT of this vector provides estimates of eigenvalues, denoted by λ_i, of the convolution matrix C. We choose a truncation parameter ζ to separate these eigenvalues, in a manner similar to that used in [11, 22]. The truncation parameter ζ is chosen so that those eigenvalues satisfying $|\lambda_i| \geq \zeta$ correspond to the signal subspace, while those satisfying $|\lambda_i| < \zeta$ correspond to the noise subspace. Thus, we set the initial estimate of the convolution matrix C to a BCCB matrix with eigenvalues

$$\tilde{\lambda}_i = \begin{cases} \lambda_i, & \text{if } |\lambda_i| \geq \zeta; \\ 1, & \text{if } |\lambda_i| < \zeta; \end{cases}.$$

In other words, we replace the eigenvalues corresponding to the noise subspace with ones, as discussed in [11] and [22]. Since the filter parameter vector corresponds to the inverse of the convolution matrix, it can be *initialized* by applying the 2-D inverse FFT to the vector of eigenvalues λ_i^{-1}.

To determine the truncation parameter ζ , we compute the discrete Fourier transform of the blurred and noisy image or the guide star image, and find the point at which the Fourier coefficients level off. The index where this stagnation begins indicates where the random errors (noise) start to dominate the blurred and noisy image or the guide star image. The value at this point is chosen as ζ. See [7], [11] or [22] for details of this procedure for estimating ζ.

4 Numerical Examples in Optical Imaging

In this section we present numerical tests of data samples to illustrate the effectiveness of our NSR-RIF algorithm approach to blind deconvolution. All the experiments are performed in MATLAB with machine epsilon $\mu \approx 10^{-16}$ precision on a Sun Ultra SPARC workstation.

Synthetic Data. The first data sample involves a degraded image of a simple known block object. This example consists of a simple 9×9 image (with 81 unknown pixel values) containing three blocks as shown in Figure 4. To obtain a blurred image, we used a Gaussian-type point spread function, shown in Figure 4, and convolved it with the original image. The blurred image is, in addition, polluted by Gaussian noise so that the resulting observed image has SNR = 10 DB, as shown in Figure 5 (left).

For our NSR-RIF algorithm, the best restoration is achieved at 9 iterations and we see from Figure 5 (right) that a visually appealing result is obtained.

For comparison purposes, the NAS-RIF algorithm suggested by Kundur and Hatzinakos [17, 18, 19] is applied to the degraded image. We see that the method converges to a good solution (Figure 6 (left) with 13 iterations), but then their scheme exhibits noise amplification on subsequent iterations (Figure 6 (right)).

In addition, Table 2 shows the corresponding relative errors for the above restored images. Our tests indicate that the NSR-RIF algorithm can effectively recover images even in the presence of high noise levels.

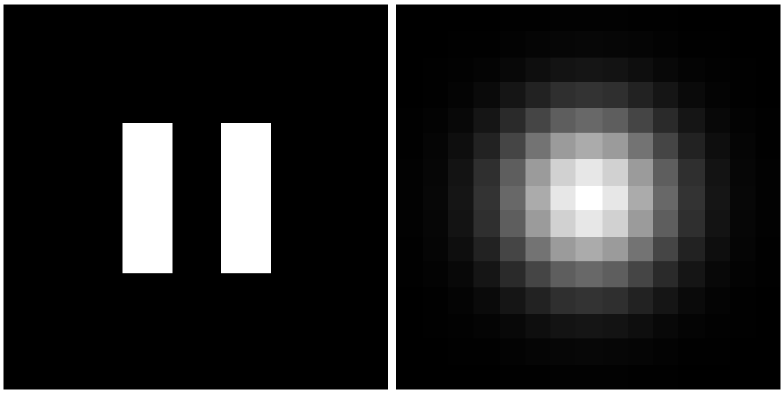

Fig. 4. Original image (left) and point spread function (right)

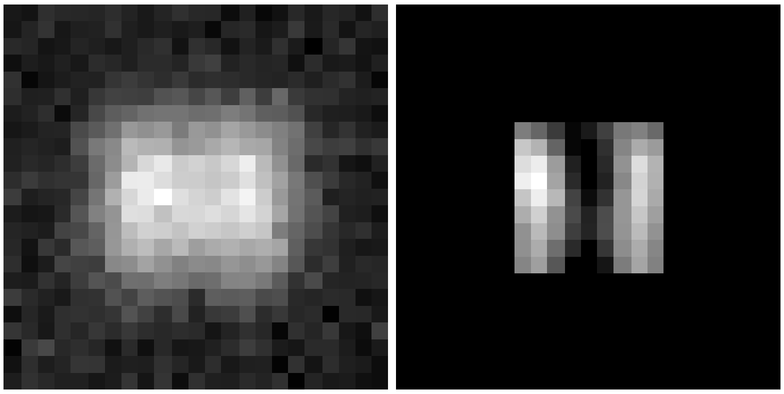

Fig. 5. Degraded image with SNR = 10 DB (left), and NSR-RIF restoration using $p = 11$, $\gamma = 0.75$, $\mu = 1.0$ and $\tau = 20$ with 9 iterations (right)

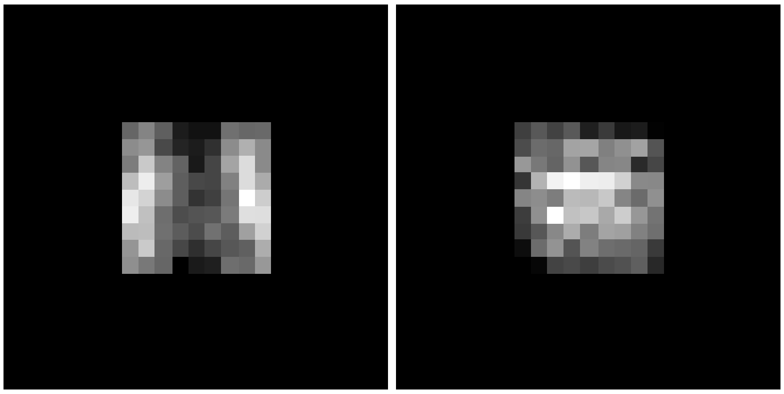

Fig. 6. For comparison purposes: NAS-RIF restoration using $p = 2$, $\gamma = 0.1$ and $\mu = 0.0$ with 13 iterations (left), and with 20 iterations (right)

The second data sample consist a synthetically generated binary text image of the letters "HK97" as shown in Figure 7 (left). To obtain a blurred image, we used a Gaussian-type point spread function shown in Figure 7 (right) and convolved it with the original image. We show that the post-processing of the image estimate given by NSR-RIF algorithm can effectively regularize the restored image. Figure 8 shows the observed image which is blurred by the Gaussian-type point spread function shown in Figure 7 (right) and is added by Gaussian noise with SNR = 50 DB. We see from Figure 9 that the post-processing procedure is useful.

Simulated Ground-Based Telescope Data. The image boundaries in Example 1 are very regular. In the next example, we consider a 256×256 image with irregular boundaries. This model problem data was obtained from the US Air Force Phillips Laboratory, Lasers and Imaging Directorate, Kirtland Air Force Base, New Mexico. This model has been used for testing various image restoration algorithms, e.g., [5, 11, 21, 22, 24, 27, 28].

Specifically, the true object is an ocean reconnaissance satellite, which is shown in Figure 10 (left). A computer simulation algorithm at Phillips Laboratory was used to produce a degraded image of the satellite, shown in Figure 11, as would be observed from a modern ground-based telescope equipped with adaptive-optics controlled deformable mirrors [24]. The satellite was modeled as being 12 meters in length and in an orbit 500 kilometers above the surface of the earth. The simulated charge-coupled device (CCD) for forming the image was a 65,536 pixel square array. CCD root-mean-square read-out noise variance was fixed at 15 microns per pixel to reflect a realistic state-of-the-art detector. In actual field experiments, several hundred measurement are averaged to reduce the effects of noise. In this example, the blurred image is polluted by noise around 30 DB. The guide star observed under similar circumstances is shown in Figure 10 (right). Notice the blur and noise in the image of the guide star, resulting in a degraded PSF.

In this example, we set the initial estimate of the 2-D convolution matrix C to a BCCB matrix with eigenvalues

$$\tilde{\lambda}_i = \begin{cases} \lambda_i, & \text{if } |\lambda_i| \geq 0.005; \\ 1, & \text{if } |\lambda_i| < 0.005. \end{cases}$$

The filter parameter vector is initialized by applying the 2-D inverse FFT to the vector of eigenvalues $1/\lambda_i$. Computed restorations by NSR-RIF algorithm (4 iterations, $\mu = 1.2$, $\tau = 120$ and $\gamma = 4.5$) using the knowledge of the guide star are shown in Figure 12. We also see that the guide star image and the support of the original image are useful in the blind deconvolution of the satellite image.

In summary, we have presented a new regularized iterative blind deconvolution method, based on recursive inverse filtering.

Preliminary numerical results indicate effectiveness of the method. Future work on this project will involve (1) testing the method on real astronomical data provided by the Air Force Phillips Laboratory Starfire Optical Range, (2)

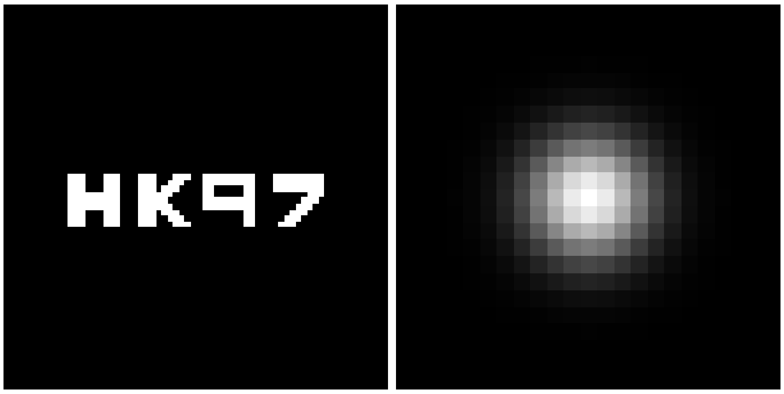

Fig. 7. Original image (left) and point spread function (right)

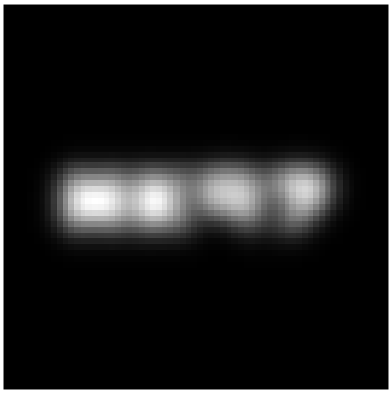

Fig. 8. Degraded image with SNR = 50 DB

Fig. 9. NSR-RIF restoration using $p = 2$, $\gamma = 0.1$, $\mu = 0.5$ and $\tau = 10$ with 68 iterations (left) and, after post-processing the image estimate (right)

incorporating the use of multiple frames of data into the algorithm, and (3) comparing the performance of our NSR-RIF algorithm with the Iterative Deconvolution Algorithm (IDAC) by Christou et al, [6, 16]. IDAC is an iterative direct filter non-linear deconvolution algorithm which, as with our NSR-RIF algorithm, uses an error metric minimisation scheme, by means of a conjugate gradient search. Their code is available, e.g., at the European Southern Observatory in Munich, Germany.

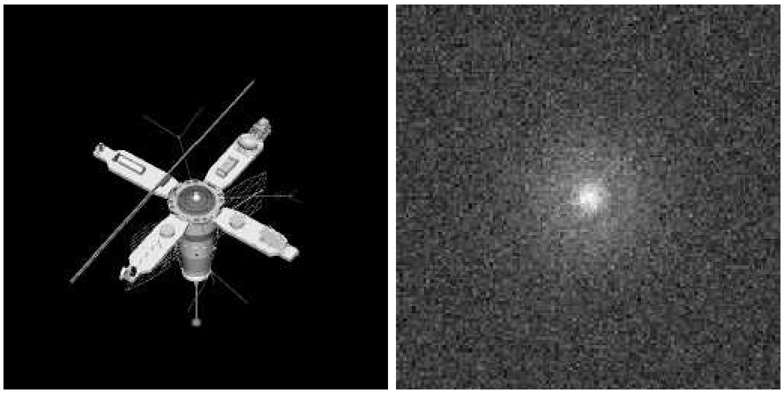

Fig. 10. Original satellite image (left) and guide star image (right)

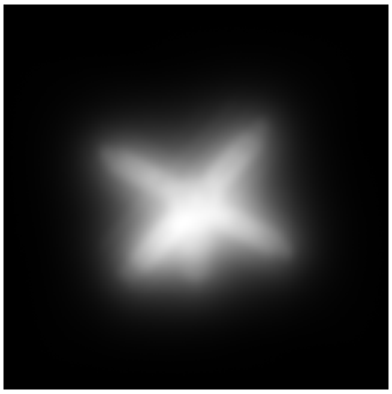

Fig. 11. Observed image

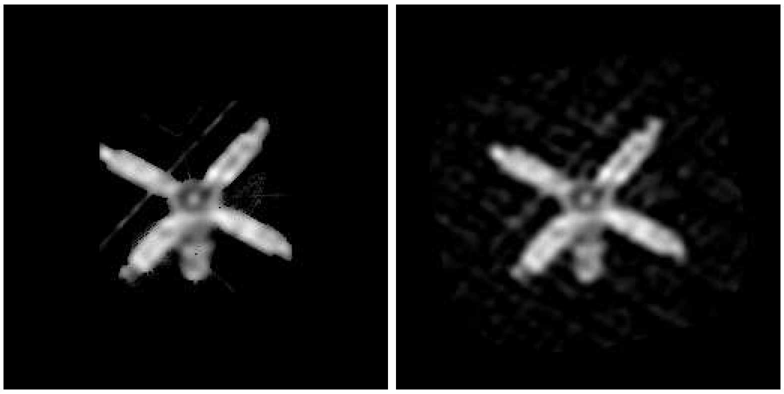

Fig. 12. Restored image with the exact support (left) and restored image with the overestimated suport (right), using the guide star image to initialize NSR-RIF

References

1. L. Alvarez and J. Morel, *Formalization and Computational Aspects of Image Analysis*, Acta Numerica (1994), pp. 1–59.
2. T. E. Bell, *Electronics and the Stars*, IEEE Spectrum 32, no. 8 (1995), pp. 16–24 .
3. A. Berman and R. J. Plemmons, *Nonnegative Matrices in the Mathematical Sciences*, 2nd Edition, SIAM Press Classics Series no. 9, Philadelphia, 1994.
4. K. Castleman, *Digital Image Processing*, Prentice–Hall, NJ, 1996.
5. T. Chan and C. Wong, *Total Variation Blind Deconvolution* , CAM Rep. 96–45, Department of Math., UCLA.
6. J. Christou, *Blind Deconvolution Postprocessing of Images Collected by Adaptive-Optics*, SPIE Proc. 2534 (1995), pp. 226–234.
7. H. Engl, M. Hanke and A. Neubauer, *Regularization of Inverse Problems*, Kluwer Academic Publishers, The Netherlands, 1996.
8. D. Fish, A. Brinicombe and R. Pike, *Blind Deconvolution by Means of the Richardson-Lucy Algorithm*, J. Optical Soc. Amer. A 12 (1995), pp. 58–65.
9. C. Groetsch, The Theory of Tikhonov Regularization for Fredholm Equations of the First Kind, Pitman Publishing, London, 1984.
10. M. Hanke and P. Hansen, *Regularization Methods for Large-scale Problems*, Surveys Math. Indust., 3 (1993), pp. 253–315.
11. M. Hanke, J. Nagy and R. Plemmons *Preconditioned Iterative Regularization for Ill–posed Problems*, Numerical Linear Algebra and Scientific Computing, Eds. L. Reichel, A. Ruttan, R. Varga, de Guyter Press, Berlin, (1993), pp. 141–163.
12. J. W. Hardy, *Adaptive Optics*, Scientific American 270, no. 6 (1994), pp. 60–65.
13. A. Houacine, *Regularized Fast Recursive Least Squares Algorithms for Adaptive Filtering*, IEEE Trans. on Signal Processing, Vol. 39, no. 4 (1991), pp. 860–871.
14. A. Houacine, *Regularized Fast Recursive Least Squares Algorithms for Finite Memory Filtering*, IEEE Trans. on Signal Processing, Vol. 40, no. 4 (1992), pp. 758–769.
15. A. Jain, Fundamentals of Digital Image Processing, Prentice-Hall, Englewood Cliffs, NJ, 1989.
16. S. Jefferies and J. Christou, *Restoration of Astronomical Images by Iterative Blind Deconvolution*, Astrophysics J., 415 (1993), pp. 862–874.
17. D. Kundur and D. Hatzinakos, *Blind Image Deconvolution*, IEEE Signal Processing Magazine, May, 1996, pp. 43–64. (See also, *Blind Image Deconvolution Revisited*, IEEE Signal Processing Magazine, November, 1996, pp. 61–63).
18. D. Kundur and D. Hatzinakos, *A Novel Blind Deconvolution Scheme for Image Restoration Using Recursive Filtering*, preprint, 1996.
19. D. Kundur and D. Hatzinakos, *On the Global Asymptotic Stability of the NAS-RIF Algorithm for Blind Image Restoration*, Proc. ICIP96, Inter. Conf. on Image Proc., Lausanne, Switzerland, September 1996.
20. R. Lagendijk and J. Biedmond, *Iterative Identification and Restoration of Images*, Kluwer Press, Boston, 1991.
21. J. Nagy, R. Plemmons and T. Torgersen, *Iterative Image Restoration using Approximate Inverse Preconditioning*, IEEE Trans. on Image Processing, 5, no. 7 (1996), pp. 1151–1162.
22. J. Nagy, P. Pauca, R. Plemmons and T. Torgersen, *Space-varying Restoration of Optical Images*, Preprint, August (1996).
23. J. Nelson, *Reinventing the Telescope*, Popular Science, 85 (1995), pp. 57–59.
24. M. Roggemann and B. Welsh, *Imaging Through Turbulence*, CRC Press, Boca Raton, FL, 1996.

25. L. Rudin, S. Osher and E. Fatemi, *Nonlinear Total Variation Based Noise Removal Algorithms*, Physica D., 60 (1992), pp. 259–268.
26. L. Rudin and S. Osher, *Total Variation Based Image Restoration with Free Local Constraints*, Proc. IEEE International Conf. on Image Processing, II (1994), pp. 31–35.
27. C. Vogel, *Solution of Linear Systems arising in Nonlinear Image Deblurring*, This Proceedings, Springer, 1997.
28. C. Vogel and M. Oman, *Iterative Methods for Total Variation Denoising*, SIAM J. Sci. Comput., 17 (1996), pp. 227–238.
29. Y. You and M. Kaveh *A Regularization Approach to Joint Blur Identification and Image Restoration*, IEEE Trans. on Image Proc., 5 (1996), pp. 416–427.

Table 1. NSR-RIF Algorithm.

Definitions:

g: the blurred and noisy signal of size k.
n: the support size.
p: the filter length is $2p+1$.
$s(t)$: the FIR filter parameter vector of dimension $2p+1$ at the t-th iteration.
$S(t)$: the corresponding matrix of the parameter vector $s(t)$ of the FIR filter.
$\tilde{y}(t)$: the estimate of the original signal at the t-th iteration.
$J_{reg}(t)$: the objective function at $s(t)$.
$\bigtriangledown J_{reg}(t)$: the gradient vector of $J_{reg}(t)$.
ϵ: the tolerance for the termination.

Initial Conditions:

Set $s(0)$ to all zeros with a unit spike in the middle,
or, to an estimate corresponding to the inverse of the PSF.

Iterations:

For $t = 0, 1, ...$
Compute $y(t) = S(t)g$.
Project $y(t)$ onto $\tilde{y}(t)$.
Compute the error $z(t) = y(t) - \tilde{y}(t)$.
Compute $\hat{s}(t) = Fs(t)$, where F is the DFT operator.
Project $\hat{s}(t)$ onto $\tilde{s}(t)$.
Compute the error $v(t) = \hat{s}(t) - \tilde{s}(t)$.
If $J_{reg}(t) < \epsilon$, **then** stop; **otherwise** compute $\bigtriangledown J_{reg}(t)$ using (13).
If $t = 0$, **then** set the conjugate gradient direction vector $d(t) = - \bigtriangledown J_{reg}(t)$;
otherwise compute $e(t) = [\bigtriangledown J_{reg}(t) - \bigtriangledown J_{reg}(t-1)]^H \bigtriangledown J_{reg}(t) / \| \bigtriangledown J_{reg}(t-1) \|_2^2$;
and set the direction vector $d(t) = - \bigtriangledown J_{reg}(t) + e(t)d(t-1)$.
Perform a line minimization to determine δ_t such that
$$J_{reg}(s(t) + \delta_t d(t)) \leq J_{reg}(s(t) + \delta d(t)), \quad \forall \delta \in \mathcal{R}.$$
Compute $s(t+1) = s(t) + \delta_t d(t)$.
End For

Table 2. Relative errors of the restored images for the NAS-RIF and NSR-RIF algorithms

y	$\|f-y\|_2/\|f\|_2$
Blurred and noisy image	0.7146
NSR-RIF restored image at 9 iterations (Figure 5)	0.4162
NAS-RIF restored image at 13 iterations (Figure 6)	0.4738
NAS-RIF restored image at 20 iterations (Figure 6)	0.7568